Collision cross sections of small water clusters

Zoltán Sternovsky, Mihály Horányi, and Scott Robertson
Physics Department, University of Colorado at Boulder, Boulder, Colorado 80309-0390
(Received 28 November 2000; revised manuscript received 20 April 2001; published 13 July 2001)

The effective integral collision cross section of small water cluster molecules, $[H_2O]_N$, with N from 4 to 8, has been measured. A controlled mixture of water vapor and argon, expanding into vacuum, produces neutral water clusters in a supersonic molecular beam. The clusters undergo collisions in a scattering cell with target gases Ar, He, or N_2, and are detected by a quadrupole mass spectrometer after electron-impact ionization. The detected cluster ions are in the form of proton hydrates $H^+[H_2O]_K$. The apparent cross sections determined from attenuation measurements are approximately of $3\times10^{-18}\,m^2$ for Ar and N_2 target gases, and $10^{-18}\,m^2$ for He. Additional data, with a beam having a smaller proportion of heavy clusters gives the same cross section for attenuation of the $K=3$ cluster, which suggests that there one dominant channel for the generation of ions from clusters.

DOI: 10.1103/PhysRevA.64.023203 PACS number(s): 36.40.Mr, 34.90.+q

I. INTRODUCTION

Noctilucent clouds (NLC's) are of interest as an indicator of water vapor in the upper atmosphere. Increased sightings of these clouds may be indicative of anthropogenic change [1,2]. These clouds are composed of water cluster molecules that become visible when they have grown to ~50 nm in radius [3–5]. Smaller clusters are thought to be associated with unusually strong radar echoes [6]. Rocket-borne mass spectrographs have detected proton hydrate cluster ions $H^+[H_2O]_N$ with $N=3-12$, which may represent the earliest stage of cloud formation [7]. Other rocket-borne instruments have detected localized reductions in electron density, "bite outs," [8] which are often seen in association with NLC's. These may arise from an attachment of electrons to the clusters [9], which is known to have a high cross section [10]. New rocket instruments have detected charged NLC particles with both signs of charge [11–13]. Modeling NLC formation [14] and the effects of cluster molecules on charge balance and ion chemistry [15] requires the knowledge of the physical properties of water cluster molecules, collision cross sections, and reaction rates. Collision cross sections are also necessary for modeling the performance of rocket-borne instruments [13,16]. In this work we describe a measurement of the effective integral cross section of water clusters $[H_2O]_N$, from $N=4$ to 8. The clusters are formed within a supersonic molecular beam, and scattered on target species: molecular nitrogen, helium, and argon.

II. EXPERIMENTAL TECHNIQUE

The experimental apparatus consist of three parts (Fig. 1). In the uppermost chamber a molecular beam containing water clusters is produced. The second chamber contains a scattering cell in which the molecular beam is attenuated by collisions. The attenuated beam is detected by a rf quadrupole analyzer in the third section, after ionization by 70-eV electrons.

The clusters are created in free-jet expansion of a mixture of argon and water vapor. A 3000-l/s diffusion pump with a water-cooled baffle maintains a vacuum of 10^{-4} Torr in the upper chamber during operation of the source. The molecular beam is collimated by a 2-mm hole in a skimmer placed 20–25 mm downstream from the 50-μm pinhole nozzle. A 450-l/s turbomolecular pump with a base pressure 2×10^{-7} Torr pumps the second chamber. There is a cylindrical scattering cell placed in the center of the second chamber, which is aligned with the molecular beam. This cell has a length $L=12$ cm and a diameter 3.5 cm. The two ends have 3-mm-diameter circular holes. A fine leak valve allows the introduction of the target gas (He, Ar, or N_2) into the scattering cell. The extra gas in the scattering cell has a negligible effect (<1%) on the pressure in the surrounding chamber. The attenuation of the cluster beam intensity by collisions outside the scattering cell can be neglected. Without gas, the pressures inside the gas cell and the surrounding chamber are equal. A standard ionization gauge is used to measure the scattering cell pressure p_{sc}, which is varied between 1×10^{-5} and 3×10^{-4} Torr. Two independent gauges located adjacent to one another gave readings that did not differ by more than 16%. In the case of helium and argon target gases, the reading from the ionization gauge was corrected with the relative gauge sensitivities: 0.18 for helium and 1.29 for argon, respectively [17]. After leaving the scattering cell, the cluster beam enters a standard commercial gas analyzer with <1-amu resolution. The analyzer consists of an ionizer, a quadrupole mass filter, and an ion detector. The ions are produced by electron impact (70 eV, 1 mA), and accelerated toward the mass filter. A channel electron multiplier is used as the detector.

The electron-impact ionization of water clusters is believed to rapidly proceed via an internal ion-molecule reaction [18],

$$[H_2O]_N+e^-\rightarrow[H_2O]_N^+ +2e^-\rightarrow H^+[H_2O]_{N-1}+OH+2e^-, \quad (1)$$

into a protonated cluster $H^+[H_2O]_{N-1}$. This reaction may be followed by evaporation of several H_2O molecules [18,19]. Thus the detected $H^+[H_2O]_K$ cluster ion intensity, I_K^+, may arise from neutral clusters with $N=K+1$, $K+2$, etc. The contribution of the $[H_2O]_N$ cluster size to a measured inten-

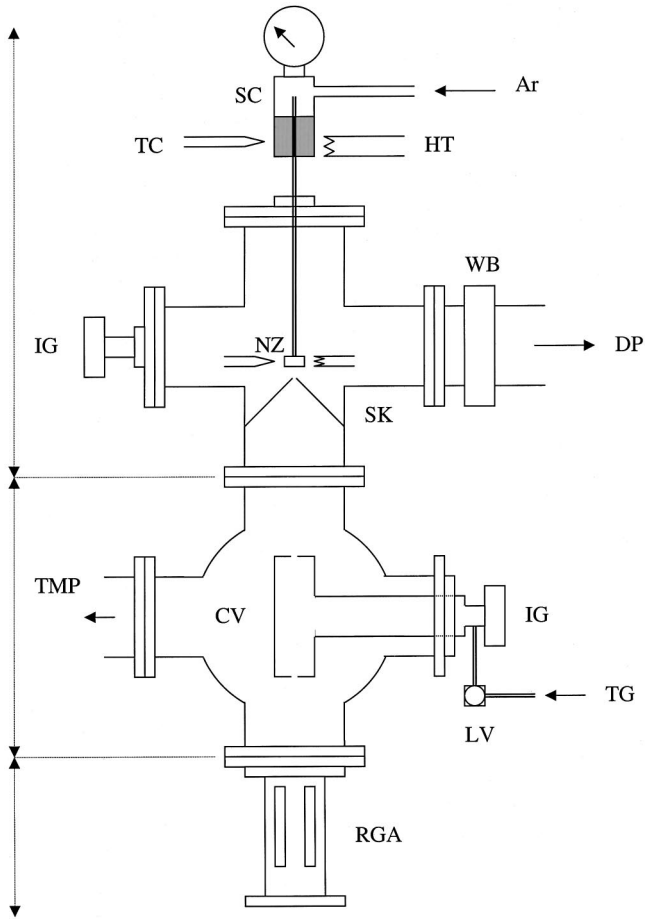

FIG. 1. The scheme of the experimental set-up. SC, stagnation chamber; Ar, argon gas inlet; TC, thermocouple; HT, heater; IG, ionization gauge; NZ, nozzle; WB, water-cooled baffle; DP, diffusion pump; SK, skimmer; TMP, turbomolecular pump; CV, collision volume; LV, leak valve; TG, target gas inlet; RGA, quadrupole residual gas analyzer.

sity I_K^+ can be expressed in terms of concentrations of neutral cluster molecules ρ_N and probabilities F_{NK} that these clusters are ionized, fragment into $H^+[H_2O]_K$, and detected $I_{N,K}^+ = F_{N,K}\rho_N$. The net intensity is then

$$I_K^+ = \sum_{N \geq K+1} I_{N,K}^+ . \tag{2}$$

Normalized values of $I_{N,K}^+$ may be introduced (marked with apostrophes), satisfying the condition

$$\sum_{N \geq K+1} I_{N,K}'^+ = 1. \tag{3}$$

The conditions within the cluster generator determine the properties of the molecular beam. At the start of the experiment, approximately 20 ml of distilled water is loaded into a heated reservoir (stagnation chamber). Its temperature is controlled by a thermocouple, and is typically kept at $T_s = 60-70\,^\circ$C. The pressure of the water vapor p_s is determined by the temperature of the stagnation chamber, and is in the range 150–250 Torr. The vapor flows to the nozzle through a copper tube. The temperature of this tube T_0 is controlled separately, and is held slightly above the reservoir temperature to avoid condensation. Argon gas is mixed with the water vapor to increase the total stagnation pressure p_{tot} to slightly above the pressure of the atmosphere (locally 620 Torr). The mixture undergoes isentropic expansion, and the temperature drops rapidly with increasing distance from the nozzle. This leads to the supersaturation of the water vapor and subsequent clustering [20].

The properties of molecular beams from free-jet expansions are well understood [20,21]. Since the nozzle-skimmer distance is large compared to the nozzle diameter, the flow entering the main chamber has a narrow velocity distribution and a large Mach number. The flow reaches terminal velocity:

$$v_i = \left[\frac{2k_B T_0}{m} \left(\frac{\gamma}{\gamma - 1} \right) \right]^{1/2}, \tag{4}$$

where k_B is Boltzmann's constant, m is the molecular weight of the expanding gas, and γ is its specific-heat ratio. In the case of gas mixtures weighted values, $\overline{m} = \Sigma X_j m_j$ and

$$\overline{\gamma/\gamma - 1} = \sum X_j (\gamma_j / \gamma_j - 1) \tag{5}$$

are used, where X_j is the mole fraction. At typical experimental conditions ($T_0 = 78\,^\circ$C, $p_s = 170$ Torr, and $p_{\text{tot}} = 700$ Torr) the mean molecular weight is 34.7 amu, giving a terminal velocity of 680 m/s for the cluster beam. The values of specific heat ratios are $\frac{5}{3}$ and $\frac{4}{3}$ for Ar and H_2O, respectively.

The cluster beam is attenuated in the scattering cell by interaction with the target gas. From the attenuation rate of intensity I_K^+, an apparent collision cross section for the average relative velocity $\overline{g}$ can be obtained using the relation

$$\sigma_{\text{app},K}^+(\overline{g}) = \frac{1}{nL} \ln \left(\frac{I_K^{0+}}{I_K^+} \right), \tag{6}$$

where I_K^{0+} is the initial flux, and $n = p_{\text{sc}}/k_B T_{\text{sc}}$ is the number density of the target gas with pressure p_{sc} and temperature T_{sc}. The target gas in the scattering cell is assumed to be homogenous with a Maxwellian velocity distribution. This apparent cross section differs from the true scattering cross section for clusters with $N = K+1$, because (1) clusters with $N > K+1$ may contribute to the detected signal, (2) of the velocity spread of the target gas molecules, and (3) very small angle collisions due not contribute to the measured attenuation [20,22]. We discuss (2) and (3) below, and discuss (1) in Sec. III, where beams of different composition are used to help unfold the contribution of heavy clusters.

Effects (2) and (3) may be separated, to a large extent, by writing the expression for the measured apparent cross section in a form [20,22]

$$\sigma_{\text{app},K}^+(\overline{g}) = \sigma_{\text{eff},K}^+(\overline{g}) - \Delta\sigma_{\text{eff},K}^+(\overline{g}), \tag{7}$$

TABLE I. The calculated properties of the colliding molecules ($\nu_i = 680$ m/s) and ϑ_{max} for three different cluster sizes $N = 4-6$.

Target gas	Mass m_k [amu]	ν_{th} (m/s)	$\overline{g}$ (m/s)	ϑ_{max} (deg) $m_i = 72$	ϑ_{max} (deg) $m_i = 90$	ϑ_{max} (deg) $m_i = 108$
Ar	40	352	766	2.6	3.1	3.5
N_2	28	420	799	3.3	3.9	4.5
He	4	1113	1304	18.0	22.3	26.6

where $\Delta\sigma^+_{\mathrm{eff},K}(\overline{g})$ represents the angular resolution correction term. In order to the angular correction, one has to calculate the portion of the cross section that is accepted by the detector and thus does not appear in the $\sigma^+_{\mathrm{app},K}(\overline{g})$. This can be done by integrating the differential cross section over the detector acceptance solid angle $\Delta\omega$ and the target gas velocity distribution ν_k in the center-of-mass system:

$$\Delta\sigma^+_{\mathrm{eff},K}(\overline{g}) = \int_{\nu_k}\int_{\Delta\omega}\frac{g}{\nu_i}\frac{d\sigma}{d\omega}f(\nu_k)d\nu_k d\omega. \tag{8}$$

From the geometry of the experimental setup, it is estimated that water clusters scattered less than $\theta_{max} \sim 1°$ full angle in the laboratory system can enter the ionizer of the mass-analyzing system. This value is a compromise between the need for angular resolution and the need for sufficient signal from the larger cluster sizes. The transformation of the laboratory deflection angle θ to center-of-mass coordinates in small-angle approximation is [20,22]:

$$\vartheta_{max}(g) = \frac{m_i}{\mu}\frac{\nu_i}{g}\left(1-\frac{\nu_{th}^2}{2g\nu_i}\right)^{-1/2}\theta_{max}, \tag{9}$$

where m_i is the mass of the projectile particles, and μ is the reduced mass of the colliding species. The most probable thermal speed of the target gas molecules with mass m_k is $\nu_{th} = \sqrt{2k_B T_{sc}/m_k}$. The calculated values of the full angle ϑ_{max} for different scattering gases at the average relative speed $\overline{g} = (\nu_i^2 + \nu_{th}^2)^{1/2}$ can be found in Table I.

The velocity resolution correction can be simply done by using the Kinsey factor $f(s,x)$, which relates the effective cross section to the true integral cross section $\sigma^+_{\mathrm{eff},K}(\overline{g}) = f(s,x)\sigma^+_K(\overline{g})\overline{g}/\nu_i$ [23]. Here x means the ratio of the beam velocity to the most probable speed of the scattering gas, and s is the power of r in the interaction potential $V(r) \sim 1/r^s$. For dipole-induced dipole interactions, $s = 6$.

III. EXPERIMENTAL RESULTS

A mass spectrum taken at typical conditions, but without a target gas is shown in Fig. 2(a). The cluster ions appear in the form of proton hydrates, $H^+[H_2O]_K$, according to Eq. (1), with $K \leqslant 10$. In addition to the cluster ions, the mass spectrum shows a variety of background peaks caused by the fragmentation of pump oils. A movable beam stop (not shown in Fig. 1) below the collision volume is used to isolate the background with experimental conditions otherwise undisturbed. Subtraction of this background gives the mass spectrum of the beam. [Fig. 2(b)]. The protonated dimer cluster ion $H^+[H_2O]_2$ was detectable in the lower mass spectrum; however, it was not suitable for accurate measurement because of nearby large background peaks. These background peaks also overlapped the lighter ionized water cluster fragments reported by Buck and Winter [19].

The drop of intensity I_K^+ with the pressure of Ar gas within the scattering cell is shown in Fig. 3 for $K = 3-7$. Each point is an average of six independent measurements, where the standard deviation is between 3% and 10%. The signal amplitude as a function of pressure shows an exponential behavior. The attenuation curves were fitted by the least-squares method, and the apparent collision cross sections $\sigma^+_{\mathrm{app},K}(\overline{g})$ were calculated from Eq. (6). The uncertainties of the measurements were deduced from the fit as well; however, these errors do not include the systematic effects. The obtained results for argon, helium, and nitrogen target gases are shown in Fig. 4 for $K = 3-7$. The values of apparent cross sections in Ar gas range from $\sigma^+_{\mathrm{app},3} = 2.87 \pm 0.08 \times 10^{-18}\,\mathrm{m}^2$ for $K = 3$ and $\sigma^+_{\mathrm{app},4} = 3.20 \pm 0.06 \times 10^{-18}$ for $K = 4$, up to $\sigma^+_{\mathrm{app},7} = 3.63 \pm 0.11 \times 10^{-18}\,\mathrm{m}^2$ for $K = 7$. The values measured in N_2 are approximately the same. The values in He are approximately $1.2 \times 10^{-18}\,\mathrm{m}^2$ for all cluster ion sizes.

In order to investigate the relative importance of fragmentations yielding ions corresponding to $N > K+1$ (signals from the fragmentation of larger clusters), additional measurements were made with a reduced fraction of heavy clusters. The partial pressure of water vapor was reduced to $p_s = 150$ Torr, with an unchanged stagnation pressure $p_{tot} = 700$ Torr, and the nozzle temperature was lowered to $T_0 = 70\,°\mathrm{C}$. At these reduced water conditions the mass spectrum of clusters decreased more rapidly with increasing K, with $K = 5$ being the largest cluster clearly observed [Fig. 2(c)]. For standard conditions, the intensity of each cluster size is approximately 0.55 of that of the cluster one size smaller, and with the reduced water content this fraction is 0.35. The beam velocity from Eq. (4) was changed by less than 2% ($\nu_i = 668$ m/s). The apparent collision cross section calculated from the attenuation measurement in Ar gas is $\sigma^+_{\mathrm{app},3} = 2.84 \pm 0.08 \times 10^{-18}\,\mathrm{m}^2$, i.e., the same as at the standard experimental conditions within the error limit. The signal intensities for $K \geqslant 4$ were not sufficient for cross-section measurements.

IV. DISCUSSION

The measured cross sections of water clusters are large compared to the naive geometric cross section. This cross

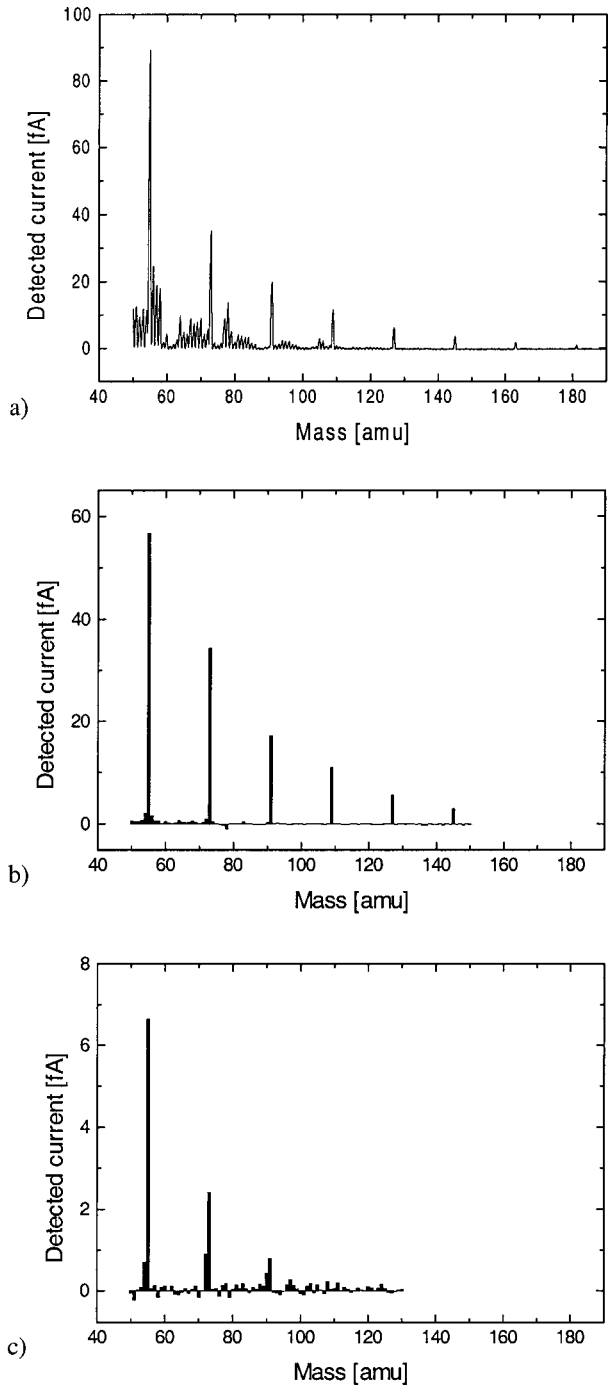

FIG. 2. (a) Typical mass spectrum. The peaks at 55, 73, 91, 109, 127, 145, 163, and 181 correspond to cluster ions $H^+[H_2O]_K$, $K=3-10$. (b) The mass spectrum with the background removed at stagnation conditions $T_0=78\,^\circ$C, $p_s=170$ Torr, and $p_{\text{tot}}=700$ Torr. (c) The mass spectrum with the background removed at stagnation conditions $T_0=70\,^\circ$C, $p_s=150$ Torr, and $p_{\text{tot}}=700$ Torr.

section for a cluster of N molecules is $\sigma_N^g=\pi(3NV_0/4\pi)^{2/3}$, where V_0 is the volume occupied by one H_2O molecule in liquid water. The cross sections σ_N^g are in the range $0.3-0.6\times10^{-18}\,\text{m}^2$ for $N=4-12$ [24]. The larger measured cross sections (about $3\times10^{-18}\,\text{m}^2$ for Ar and N_2 target gases, and $1.2\times10^{-18}\,\text{m}^2$ for He) are most likely a result of a long-range interaction [25]. This interaction is from van der Waals forces (dipole-induced dipole interaction) between the polar H_2O molecules (dipole moment $\mu=1.855$ D, where $\text{D}=3.336\times10^{-30}$ C/m is the Debye unit) in the cluster and the polarizable target gases that is $\alpha_{\text{He}}=0.22\times10^{-40}\,\text{J}^{-1}\,\text{C}^2\,\text{m}^2$, $\alpha_{\text{Ar}}=1.85\times10^{-40}\,\text{J}^{-1}\,\text{C}^2\,\text{m}^2$, $\alpha_{N_2}=1.97\times10^{-40}\,\text{J}^{-1}\,\text{C}^2\,\text{m}^2$ for He, Ar, and N_2, respectively [26].

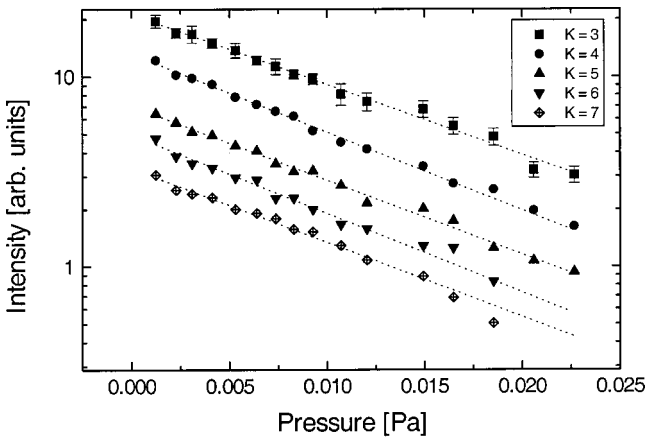

FIG. 3. The semilogarithmic plot of the cluster intensity as a function of the collision volume pressure for the case of Ar target gas. The error bars represent the standard deviation from six measurements.

In Fig. 4 there is the expected trend of increasing cross sections with increasing size K of water cluster ions for the Ar and N_2 target gases. In the case of He target gas, the relatively constant apparent cross section may be explained by the larger mass ratio and the finite acceptance angle of the analyzer. As the cluster size N increases, the collisions with the lighter He atoms result in a smaller deflection angle according to Eq. (9). The angular correction is less significant for Ar and N_2. The velocity correction of the cross section is independent of the mass.

An interesting feature that appears on Fig. 4 is a discon-

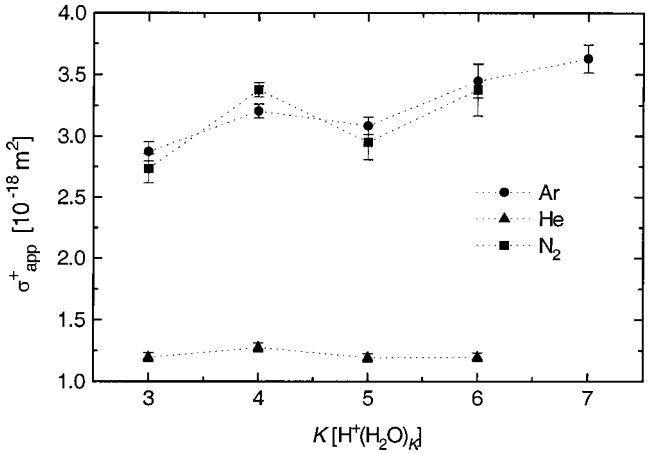

FIG. 4. The apparent collision cross sections of water cluster ions $K=3-7$ in Ar, and $K=3-6$ in He and N_2 gases.

tinuity (dip) in the cross section for all target gases at the protonated water pentamer, $H^+[H_2O]_5$. In comparing cross sections for different cluster sizes, the systematic measurement errors (~20% from the pressure measurements, for example) are the same. This effect indicates a smaller apparent cross section for the precursor molecule. Recent theoretical calculations and vibration-rotation tunneling experiments [27,28], suggested that, in free expansion, the most stable water tetramer and pentamer have a two-dimensional cyclic structure, and the most stable form of the of the water hexamer is a cage structure. If the ion $H^+[H_2O]_5$ arises primarily from impact ionization of the hexamer, the smaller cross section may be the result of the tighter geometrical configuration. This cluster ion is one of the earlier observed ''magic numbers'' that are seen as discontinuities in the mass spectra of water clusters [29,30].

Because of the possible fragmentation, there is no straightforward connection between the detected cluster ions $H^+[H_2O]_K$ and their parental neutral clusters $[H_2O]_N$. The measured cross section $\sigma^+_{\mathrm{app},K}(\overline{g})$ can be expressed as a weighted sum of all the contributing neutral clusters cross sections

$$\sigma^+_{\mathrm{app},K}(\overline{g}) = \sum_{N \geqslant K+1} I'^+_{N,K} \sigma_{\mathrm{app},N}(\overline{g})$$

according to Eq. (3). The fragmentation upon electron impact was recently studied by Buck and Winter [19] on water cluster molecules with $N \leqslant 4$. The main fragment channels for $N=3$ and 4 water clusters were found to be according to Eq. (1) with a subsequent evaporation of one water molecule from the ion. There appear to be no data investigating the fragmentation of clusters larger than $N=4$. This evaporation is a consequence of excess energy gained from the exothermic ion molecule reaction [Eq. (1)], the geometrical rearrangement occurring within the ion, and the excitation of vibration modes by the impacting electron. The excess energy from $N \geqslant 3$ clusters is primarily removed by evaporation of monomer units [19]. The binding energy of a monomer in cluster ion $H^+[H_2O]_K$ decreases with increasing K from about 1.47 eV for $K=2$ to 0.74 eV for $K=4$ [19,31]. It was suggested by Buck and Winter [19] that there is an increasing tendency for evaporation of more than one water monomer is increasing with cluster size because of the decreasing binding energy. However, with increasing size the internal degrees of freedom also increase. The excess energy then may be distributed into vibrational modes. The apparent cross sections for $H^+[H_2O]_3$ measured with beams having differing proportions of heavy clusters were found to be identical within the error. These data suggest that there is a single dominant channel contributing to the cross section. The lower cross section at $K=5$ suggests that its origin is the $N=6$ cluster.

ACKNOWLEDGMENTS

The present work was supported by the Department of Energy (Fusion Energy Sciences). We thank Zdeněk Herman, Veronica Vaida, and Shawn M. Kathmann for their useful comments, and Matt Triplett for his technical assistance.

[1] G. E. Thomas, Adv. Space Res. **18**, 149 (1996).
[2] G. E. Thomas, J. Atmos. Terr. Phys. **58**, 1629 (1996).
[3] G. E. Thomas and C. P. McKay, Planet. Space Sci. **33**, 1209 (1985).
[4] G. von Cossart, J. Fiedler, and U. von Zahn, Geophys. Res. Lett. **26**, 1513 (1999).
[5] M. Alpers, M. Gerding, J. Höffner, and U. von Zahn, J. Geophys. Res. **105**, 12235 (2000).
[6] J. Y. N. Cho and J. Röttger, J. Geophys. Res. **102**, 2001 (1997).
[7] L. G. Björn, E. Kopp, U. Hermann, P. Eberhardt, P. H. G. Dickinson, D. J. Mackinnon, F. Arnold, G. Witt, A. Lundin, and D. B. Jenkins, J. Geophys. Res. **90**, 7985 (1985).
[8] B. Inhester, J. C. Ulwick, J. Cho, M. C. Kelley, and G. Schmidt, J. Atmos. Terr. Phys. **52**, 855 (1990).
[9] U. von Zahn and J. Bremer, Geophys. Res. Lett. **26**, 1521 (1999).
[10] M. Knapp, O. Echt, D. Kreisle, and E. Recknagel, J. Phys. Chem. **91**, 2601 (1987).
[11] O. Havnes, J. Trøim, T. Blix, W. Mortensen, L. I. Næeshim, E. Thrane, and T. Tønnesen, J. Geophys. Res. **101**, 10839 (1996).
[12] L. J. Gelinas, K. A. Lynch, M. C. Kelly, S. Collins, S. Baker, Q. Zhou, and J. S. Friedman, Geophys. Res. Lett. **25**, 4047 (1998).
[13] M. Horányi, S. Robertson, B. Smiley, J. Gumbel, G. Witt, and B. Walch, Geophys. Res. Lett. **27**, 3825 (2000).
[14] T. Sugiyama, J. Geophys. Res. **99**, 3915 (1994).
[15] G. C. Reid, J. Geophys. Res. **94**, 14 653 (1989).
[16] M. Horányi, J. Gumbel, G. Witt, and S. Robertson, Geophys. Res. Lett. **26**, 1537 (1999).
[17] R. L. Summers, NASA Tech. Note TN D-5285, Lewis Research Center, National Aeronautics and Space Administration (unpublished).
[18] F. Huisken, M. Kaloudis, and A. Kulcke, J. Chem. Phys. **104**, 17 (1996).
[19] U. Buck, M. Winter, Z. Phys. D: At., Mol. Clusters **31**, 291 (1994).
[20] *Atomic and Molecular Beam Methods*, edited by G. Scoles (Oxford University Press, New York, 1988), Vol. 1, Chap. 2, pp. 19.
[21] J. B. Anderson and J. B. Fenn, Phys. Fluids **8**, 780 (1965).
[22] J. W. Bredewout, C. J. van den Meijdenberg, and J. J. M. Beenakker, Physica A **85A**, 28 (1976).
[23] N. C. Lang, H. V. Lilenfeld, and J. L. Kinsey, J. Chem. Phys. **55**, 3114 (1971).
[24] A. A. Vostrikov, D. Yu. Dubov, and M. R. Predtechenskii, Zh. Tekh. Fiz. **57**, 760 (1987) [Sov. Phys. Tech. Phys. **32**, 459 (1987)].
[25] O. V. Vasilev and H. Reiss, J. Chem. Phys. **105(7)**, 2946 (1996).
[26] P. W. Atkins, *Physical Chemistry*, 5th ed (Oxford University Press, Oxford, 1994), p. 753.

[27] K. Liu, M. G. Brown, C. Carter, R. J. Saykally, J. K. Gregory, and D. C. Clary, Nature (London) **381**, 501 (1996).
[28] J. K. Gregory, D. C. Clary, K. Liu, M. G. Brown, and R. J. Saykally, Science **275**, 814 (1997).
[29] V. Hermann, B. D. Kay, and A. W. Castleman, Jr., Chem. Phys. **72**, 185 (1982).
[30] D. Dreyfuss and H. Y. Wachman, J. Chem. Phys. **76**, 2031 (1982).
[31] K. A. Cowen, B. Plastridge, D. A. Wood, and J. V. Coe, J. Chem. Phys. **99**, 3480 (1993).